Can dynamic imaging, using 18F-1 FDG PET/CT and CT perfusion differentiate between benign and malignant pulmonary nodules?

Can dynamic imaging, using 18F-FDG PET/CT and CT perfusion differentiate between benign and malignant pulmonary nodules?

Aleksander Marin [a,c], John T Murchison [b], Kristopher Skwarski [b], Adriana A. S. Tavares [a], Dilip Patel [c], Alison Fetcher [a], William Walker [d], William Wallace [e], Vladka Salapura [f], Edwin J.R. van Beek [a], Saeed Mirsardraee [a,g]

a Edinburgh Imaging facility Queens Medical Research Institute, University of Edinburgh, Edinburgh, United Kingdom, b Departments of Respiratory Medicine, c Radiology, d Thoracic Surgery, and e Pathology Royal Infirmary of Edinburgh, Edinburgh, United Kingdom, f Faculty of Medicine, University of Ljubljana, Ljubljana, Slovenia, g National Lung and Heart Institute, Imperial College London, United Kingdom

Introduction

Pulmonary nodules are detected with increasing frequency due to widespread use of computed tomography (CT).[1,2] The prevalence of incidental pulmonary nodules on standard CT studies is around 13%, while lung cancer screening will detect lung nodules in up to 53% of subjects, leading to a lung cancer prevalence of around 1.4% (0.5–2.7%).[3] The optimal diagnostic approach for the management of indeterminate pulmonary nodules has been the subject of much discussion.[4]

The widely accepted guidelines published by the British Thoracic Society (BTS) and the Fleischner Society recommend the minimum nodule diameter

thresholds and CT follow-up time intervals for surveillance of solitary nodules smaller than 8 mm.[3,5] For nodules of ≥8 mm (300 mm^3), the BTS guidelines recommend risk assessment using the Brock model. The above guidelines recommend either 3-month CT follow-up, work-up with positron emission tomography (PET) with 2-deoxy-2-[fluorine-18]fluoro-D-glucose (^{18}F-FDG), tissue sampling, or resection for nodules of ≥8mm. CT characterisation using only morphological features is imprecise,[6,7] leading to an increased interest in computer-based radiomics assessment.[8–15] Serial CT imaging to monitor nodule size can be problematic as nodule growth varies with different cancers and causes patient anxiety.[16–18] ^{18}F-FDG PET has high sensitivity but lower specificity of 82% for detecting malignant pulmonary nodules, particularly in those smaller than 10 mm.[19] Imaging guided sampling of small nodules is also difficult, is associated with complications, and its diagnostic yield decreases further as nodule size decreases.[3,20,21]

Neovascularisation is a complex process known to be central to carcinogenesis.[22] Advances in the imaging technology in the last two decades have enabled the study of perfusion characteristics within pulmonary nodules.[23–27] As benign and malignant lesions have different vascularity, different perfusion parameters and dynamic ^{18}F-FDG uptake properties can be expected.[27–32]

The purpose of this pilot study was to evaluate the feasibility and accuracy of CT perfusion and dynamic ^{18}F-FDG PET imaging in differentiating proven benign and malignant pulmonary nodules.

Materials and methods

This single-centre prospective study was approved by the local Research Ethics Committee (13/SS/0153) and written informed consent was obtained from all participants.

Between December 2014 and December 2015, 20 consecutive patients who were referred to our respiratory outpatient clinic for an indeterminate incidental pulmonary nodule were recruited. The inclusion criteria were: a) incidentally detected soft tissue (solid) pulmonary nodules measuring $\geq$8 mm and <30 mm on CT, b) either surgical excision, imaging guided biopsy or imaging follow up of the nodule planned. The exclusion criteria were: a) abnormal renal function, b) previous adverse reaction to iodinated contrast agent, c) known history of malignancy, d) pregnancy or breast feeding, e) patients who refused or were unable to provide informed consent.

The patients underwent a dynamic ^{18}F-FDG PET/CT and dynamic perfusion CT imaging within a 3 week time frame (mean, 6.4 days: range 1–18 days). Due to technical reasons, the dynamic PET data could not be used in 4 patients for the analysis, one of these patients had two synchronous nodules. CT perfusion analysis was performed in 17 of the nodules. One patient declined the CT perfusion scan and 3 patients had significant breathing artefact on the scans, rendering analysis non-feasible. All nodules were classified into either benign or malignant on the basis of a histopathological diagnosis (n=16), or stability during 2 years follow up CT imaging (n=5).

Dynamic PET/CT image acquisition:

All patients were fasted for at least six hours before the imaging. Following a low dose CT scan for attenuation correction and localisation (120 kV, 50 mAs, 5/3 mm), patients were administered 400 MBq of ^{18}F-FDG intravenously, and a dynamic 60 minute image acquisition was performed using a Siemens Biograph PET/CT scanner (Siemens Healthcare, Erlangen, Germany). Respiratory-gated PET data were reconstructed using a 15-frame protocol (7 frames×180 s, 7×300 s, 1×240 s), a matrix size of 256×256×53 with a voxel size of 2.65×2.65×3.00 mm^3, and subsets expectation maximization (OSEM) method. A conventional PET/CT scan was performed on completion of the dynamic phase of the scan at 1 hour after injection of the tracer.

Perfusion volume CT acquisition:

Dynamic perfusion CT scans were performed as previously described [25,28,33,34] on a 320-detector row CT scanner (Aquilion ONE; Toshiba Medical Systems, Tokyo, Japan) with 16 cm field of view coverage. Imaging was performed at 0, 2, 4, 6, 8, 10, 12, 14, 16, 18, 20, 24, 30, 40, 50, 60, 90, 120 seconds, 3 minutes, 4 minutes, and 10 minutes following the intravenous injection of 70 ml of iodinated contrast (Iomeron 400 mg/ml, Bracco, Milan, Italy) followed by a 30 ml bolus of saline both at 9 ml/s through a 16 G cannula sited in the ante cubital fossa. Acquisition parameters were 100 kV, 100 mA, 0.5 seconds rotation time, 320 x 0.5 mm collimation, 512 x 512 matrix.

Image Analysis:

Dynamic PET/CT:

Reconstructed images were imported into PMOD 3.409 software (PMOD Technologies, Zurich, Switzerland) and the input function was determined by placing a spherical volume of interest (VOI) with diameter of 1 cm in the ascending aorta. VOIs were drawn around the pulmonary nodules semi-automatically with a threshold of 50% of the maximum voxel value within the nodule, and then the VOIs were copied to the dynamic imaging sequence to obtain the time activity curves (TACs) (Figure 1). The influx constant K_i (min^{-1} or (ml plasma)*(ml tissue)$^{-1}$*min^{-1})) was determined by Patlak analysis.[35] The Patlak plot model is a graphical analysis technique based on a 2-tissue compartment model with irreversibly trapped tracer. A mathematical transformation of the tissue compartment and plasma TACs produces a straight line plot which provides information about the blood volume (BV) of the tissue compartment and the exchange rate (K_i) (Figure 2).

Conventional PET/CT scan:

The maximum standardised uptake value (SUV_{max}) was measured for each nodule on conventional FDG PET/CT images. For the semi-quantitative analysis, the mean standardised uptake values (SUV_{mean}) were measured of the ascending aorta at the level of the arch, and within the right lobe of the liver. SUV ratios (SUR) were calculated between the nodule SUV_{max}, and the SUV_{mean} of the mediastinal blood pool (SUR_{BLOOD}) and liver (SUR_{LIVER}). Criteria for malignancy were specified as SUV_{max} ≥2.5; SUR_{BLOOD} ≥1.56; SUR_{LIVER} ≥1.12. Qualitative assessment PET features were specified as following: 0 = no visible uptake; 1 = uptake less than mediastinal blood pool; 2 = uptake comparable to mediastinal blood pool; 3 = uptake greater

than mediastinal blood pool; 4 = distant metastases. Qualitative specified criteria for malignancy was PET grade ≥ 3.[36,37] Volumes of interest (VOIs) were placed over the nodules, the ascending aorta at the level of the arch, and within the right lobe of the liver for determination of the SUV_{mean} and SUV_{max} values using OsiriX software (OsiriX, version 8.0.1 64 bit; OsiriX Imaging Software, Geneva, Switzerland).

Perfusion CT:

Perfusion analysis was performed using Body Perfusion Application on a Vitrea Workstation (Vitrea fX 6.0; Vital Images, Minnetonka, MN, USA). Regions of interest (ROIs) were placed over the pulmonary nodules and contralateral lung parenchyma (diameter range, 7–29 mm) on all perfusion CT images. Arterial input was determined by placing 1 cm ROI over the main pulmonary artery. Time-density graphs were then reviewed and adjustments to start point and end point of the maximum slope were made if needed to define the optimal slope range. Arterial flow perfusion maps overlaying CT images were visually analysed and ROIs were placed over the nodules to obtain the equivalent blood volume parameter calculated by Patlak plot model (BV, expressed in ml per 100 ml) and Arterial Flow (AF, expressed in ml per 100g per minute) using single-input maximum slope model for calculation.

Statistical Analysis:

All results were expressed as mean ± standard deviation (SD) unless indicated. K_i and perfusion indices BV and AF of benign and malignant nodules were statistically compared using the nonparametric Mann-Whitney U

149 test. The accuracy of the different techniques and parameters was tested with
150 area under the curve (AUC) in receiver operating characteristic (ROC)
151 analysis with 95% confidence interval (CI). Comparison between the ROCs
152 was performed using DeLongs test. Youdin index analysis was used to derive
153 the optimised cut-point values. Mann-Whitney U test and ROC curve analyses
154 were performed on GraphPad Prism version 8.2.1 for Windows (GraphPad
155 Software, San Diego, CA, USA). Youdin index analysis and nonparametric
156 DeLongs test were performed on MedCalc Statistical Software version 19.8
157 (MedCalc Software Ltd, Ostend, Belgium; https://www.medcalc.org; 2021). A
158 p value < 0.05 was considered statistically significant.

Results

The demographic data, average nodule size, SUV_{max}, metabolic parameter relating to the pulmonary nodules through dynamic ^{18}F-FDG PET/CT, and perfusion parameters through perfusion CT for the benign and malignant nodules are summarised in Table 1 and Fig 3. We analysed 21 soft tissue nodules in 20 patients (male/female=11/9; mean age±SD: 65.3±7.4; age range: 50–76 years) with mean nodule diameter±SD of 20.1±7.5 mm (9–29 mm); mean nodule volume±SD: 2849±2338.7 mm^3 (247–9348 mm^3). 52% of the nodules were located in the upper lung lobes (right upper lobe 7/21, left upper lobe 4/21), 48% were in middle and lower lung lobes (right middle lobe 2/21, right lower lobe 6/21 and left lower lobe 2/21). Final diagnosis was determined after surgical resection in 10 patients, core CT guided biopsy or bronchoscopy in 6 patients, and over 2 years stability on follow up CT imaging in 5 patients.

As shown in Table 1 and Fig 3, SUV_{max} derived from the conventional ^{18}F-FDG PET/CT and K_i derived from dynamic ^{18}F-FDG PET/CT were significantly higher in malignant nodules than in benign nodules. Also, the Patlak model derived BV on perfusion CT was significantly higher in malignant nodules. The difference in AF between the benign nodules and malignant nodules was not statistically significant.

The benign outlier on ^{18}F-FDG PET/CT (SUV_{max}=6.3) and dynamic ^{18}F-FDG PET/CT (K_i=0.0179 min^{-1}) was an 18 mm nodule of inflammation and fibrosis (Fig 3 (a) and (b)). The perfusion CT indices BV and AF in this nodule were relatively low, 3.8 ml/100ml and 51.5 ml/100g/min, respectively (Fig 3 (c) and

(d)). The two malignant outliers on conventional ^{18}F-FDG PET/CT and dynamic ^{18}F-FDG PET/CT were 12 mm and 16 mm mucinous adenocarcinomas *in situ* (12 mm nodule with SUV_{max}=0.7 and K_i=0.0015 min^{-1} (BV and AF analysis non-feasible due to respiratory motion artefact); 16 mm nodule with SUV_{max}=1.0, K_i=0.0033 min^{-1}, BV=48.8 ml/100ml and AF=154.1 ml/100g/min) (Fig 3 (a) and (b)). The mean CT densities of these two nodules on unenhanced CT images were 16.3HU and 15.9HU, while the mean density ± SD of all benign and malignant nodules analysed was 24.55±12.01 HU. The benign outlier in AF on perfusion CT was a 10 mm perivascular epithelioid cell tumour (PEComa), AF=272.7 ml/100g/min (Fig 3 (d)). The BV in this nodule was 20.5 ml/100ml, the ^{18}F-FDG PET/CT indices were low, SUV_{max}=0.7 and the K_i=0.001 min^{-1}.

Table 2 and Figure 4(a) show diagnostic accuracy of conventional PET/CT derived parameters with pre-specified and derived cut-point values though ROC analysis.[36,37] SUR_{BLOOD} parameter had overall highest accuracy, however, pairwise comparison of AUCs showed no significant difference (p = 0.5308 vs SUV_{max}; p = 1.0000 vs SUR_{LIVER}; p =0.1083 vs PET grade). ROC analysis and diagnostic accuracy for the diagnosis of malignancy by dynamic ^{18}F-FDG PET/CT parameter K_i, and perfusion CT indices BV and AF compared to SUR_{BLOOD} are further detailed in Table 2 and Figure 4(b). Pairwise comparison of AUCs of SUR_{BLOOD}, K_i, BV and AF showed no significant difference in their diagnostic performances (p > 0.1 for all comparisons).

Discussion

Our results demonstrate that the metabolic parameter K_i of dynamic ^{18}F-FDG PET/CT and the BV parameter of perfusion CT are significantly lower in benign nodules.

Our study showed that the diagnostic accuracy of the conventional ^{18}F-FDG PET/CT was best when semi-quantitative assessment and measuring the uptake ratio of the lung nodule to the mediastinal blood pool with cut-point criteria for malignancy SUR_{BLOOD} ≥1.56 was used. This has been confirmed in a larger multicenter trial by Evangelista *et al*.[36] Different to the SPUTNIK trial which has shown SUV_{max} to be the most accurate and reproducible technique with a caveat of introducing additional cut-point values altered according to the nodule size, we did not see significant improvement in diagnostic accuracy when replicating the multiple cut-points in our group of nodules (see * in Table 2).[37]

The accuracies of the new metabolic parameter K_i and perfusion parameter BV were not significantly different to the conventional ^{18}F-FDG PET/CT. The derived K_i cut-point for malignancy was ≥0.01 min^{-1} resulting in sensitivity/specificity/accuracy of 77.8%/85.7%/81.3%, respectively. This is in good agreement with K_i cut-point ≥0.014 min^{-1} reported in the study by Huang *et al*. (n=35).[26] The derived BV cut-point value of ≥21 ml/100ml for malignancy showed comparable diagnostic accuracy to conventional and dynamic ^{18}F-FDG PET/CT parameters. The high specificity of BV demonstrated in our nodules would need to be confirmed in larger studies.

The benign outlier on dynamic ^{18}F-FDG PET/CT with a high K_i parameter histopathologically represented inflammation (Fig 3 (b)). Higher metabolic activity is not only a feature of malignant cells, it can be observed in inflammatory nodules due to increased glucose metabolism in granulocytes and macrophages in a range of diseases, including fungal and necrobiotic rheumatoid nodules, sarcoidosis, tuberculosis, and other granulomas.[38,39] Dual time PET/CT did not prove to be useful for differentiating benign and malignant pulmonary nodules with an SUV_{max} less than 2.5 in regions with high prevalence of granulomatous disease.[40,41] Huang *et al.* showed that dynamic ^{18}F-FDG PET/CT is valuable in differentiating benign from malignant pulmonary nodules with the potential to differentiate malignant from granulomatous disease.[26] Our study showed limited diagnostic accuracy of the dynamic ^{18}F-FDG PET/CT in assessing inflammatory nodules.

The malignant outliers on dynamic ^{18}F-FDG PET/CT with low K_i parameters were histopathologically mucinous adenocarcinoma *in situ*. Other malignant nodules in which low metabolic activity can be measured on ^{18}F-FDG PET/CT are minimally invasive adenocarcinoma, carcinoid, and lung lymphoma.[38,42] Another important finding was that both malignant nodules with low metabolic activity were of lower CT density analysed on the initial perfusion CT images but also appreciable on low-dose CT scan of PET/CT examination. Further studies on low density lung nodules are needed for evaluation of using lower cut-point values for malignancy in conventional and dynamic PET/CT. Malignant lung nodules with low CT density and measuring less than 1 cm are known to have low metabolic activity on conventional ^{18}F-FDG PET/CT.[43,44] Berger *et al.* have reported up to 41% of lung lesions to be false-negative on

conventional ^{18}F-FDG PET/CT in analysis of 25 mucinous, hypocellular lung lesions (3/9 false negative lesions were ≤ 2 cm, range, 1–5 cm).[45] Our study showed a limited diagnostic accuracy of the dynamic ^{18}F-FDG PET/CT in assessing low density malignant pulmonary nodules with K_i cut-point set at 0.01 min^{-1}.

Dynamic enhancement CT studies help identify false positive results in both inflammatory and infective conditions, and sometimes in benign vascular tumours.[46,47] The perfusion CT parameters for the inflammatory nodule in our study were low and indicative of a benign lesion despite high metabolic activity on ^{18}F-FDG PET/CT. We have shown that the parameters of perfusion CT of both malignant nodules with low metabolic activity were higher than the BV and AF in benign nodules. Therefore, our findings indicate parameters of perfusion CT may aid in the identification of benign nodules with high glucose metabolic activity and in the identification of malignant nodules with low glucose metabolic activity. Ohno *et al.* have shown that perfusion CT is more specific and accurate than conventional ^{18}F-FDG PET/CT.[24,29] Our study on a small sample of cases suggests that perfusion CT also performs better than dynamic ^{18}F-FDG PET/CT.

The AF parameter of the perfusion CT obtained by the maximum slope method was not significantly different between benign and malignant nodules. Benign nodules had a lower AF parameter value than malignant nodules overall with one significant benign outlier with markedly high AF. Histopathologically, this represented an extremely rare ‘light cell’ or ‘sugar type’ PEComa. There are only about 50 cases of this neoplasm described in

the literature.[48,49] PEComas are more commonly found as angiomyolipomas in the kidneys, or as lesions in the retroperitoneal space, gastrointestinal tract, or uterus. Only 7 cases of malignant pulmonary PEComa have been reported [50]. A case report of a benign pulmonary PEComa showing early wash-in enhancement with an early washout pattern of a malignant lesion on perfusion CT has been reported by Kim *et al*.[51] Despite a markedly high AF, the PEComa had a BV just under the cut-point value for malignancy and a low metabolic parameter K_i of dynamic ^{18}F-FDG PET/CT. The BV parameter in combination with low K_i parameter proved to be more reliable for defining this extremely rare histological type of a pulmonary nodule.

Our study has limitations. This pilot study was performed in a small sample of patients and appropriately powered studies will be required for further validation. The mean nodule size was 18 mm for benign and 22 mm for malignant nodules, which would not normally be referred for imaging follow-up. The BTS and Fleischner Society recommended lower thresholds for nodule follow up (5mm and 6mm, respectively). More novel reconstruction methods in PET/CT such as specific point spread function (PSF) are enabling better spatial resolution and enable its use in 6 mm pulmonary nodules.[52]

Perfusion CT is quite demanding on patients with a prolonged breath-hold, which limits the availability of reliable data in some patients. All 3 nodules in which analysis was non-feasible due to the significant breathing artefact were near the diaphragm (2 in the right lower lobe and 1 in the right middle lobe). Segmentation of the pulmonary nodules on image analysis is restricted when the images were affected by respiratory motion artefact, especially in small

303 nodules which were also abutting the chest wall or mediastinal structures.
304 Some authors recommend quiet breathing during the perfusion CT scans but
305 this is only acceptable in larger lung masses.[53] There is a need for further
306 optimisation of nodule segmentation and advanced image registration
307 techniques that allow accurate assessment of pulmonary nodules without
308 need for long breath-hold.[23,54] The effective radiation dose for dynamic ^{18}F-
309 FDG PET/CT was around 8 mSv and for perfusion CT around 20 mSv. The
310 radiation dose for perfusion CT can be improved by reducing the field of view
311 from 16 cm to the nodule only and reducing tube voltage in smaller size
312 patients.[55]

313 Potential increase in the demand for these not widely available novel dynamic
314 imaging studies would consequently put additional strain on the imaging
315 departments with increased demand for scanner time, funding and training of
316 the staff. Limited capacity for a wider use of the dynamic imaging in lung
317 nodules could be overcome by developing systems of identification of nodules
318 with highest diagnostic benefit from dynamic imaging. A multicentre
319 prospective cohort observational study initiated in 2016 is set to assess the
320 performance and the cost-effectiveness of the dynamic CT and PET/CT in the
321 characterisation of solitary pulmonary nodules.[56]

322 The small sample size limits the assessments of accuracy in our study.
323 However, on this small sample we showed increase diagnostic improvement
324 in the accuracy of diagnosis in both dynamic studies when compared to the
325 conventional ^{18}F-FDG PET/CT. Specificity in K_i and BV on our small sample

size were higher at the estimated threshold values of 0.01 min^{-1} and 21 ml/100ml, respectively. This would need to be confirmed in larger studies.

Early identification of a lung nodule as benign or malignant by analysing its metabolic and perfusion parameters could reduce the need for CT to monitor lung nodule size, thereby reducing the number of CT scans required. It could also reduce the need for CT guided biopsy or other invasive procedures. Patients with malignant lung nodules could thus be identified more quickly and referred for radical treatment. With our study, we have demonstrated the potential of perfusion CT. The BV parameter assessed by perfusion CT was not only significantly lower in benign nodules, it also aided in correctly characterising the metabolically active inflammation, hypervascular benign PEComa and low density malignancy.

In conclusion, this study demonstrated the feasibility of dynamic ^{18}F-FDG PET/CT and CT perfusion studies in differentiating benign and malignant pulmonary nodules. The dynamic ^{18}F-FDG PET/CT and perfusion CT derived blood volume can assist to differentiate benign and malignant lung nodules and in indeterminate cases, a combined approach can be helpful.

References

1. Furtado CD, Aguirre DA, Sirlin CB, Dang D, Stamato SK, Lee P, et al. Whole-body CT screening: Spectrum of findings and recommendations in 1192 patients. Radiology. 2005;237(2):385–94.

2. Brenner DJ, Hall EJ. Computed Tomography — An Increasing Source of Radiation Exposure. N Engl J Med. 2007 Nov 29;357(22):2277–84.

3. Callister MEJ, Baldwin DR, Akram AR, Barnard S, Cane P, Draffan J, et al. British thoracic society guidelines for the investigation and management of pulmonary nodules. Thorax. 2015;70:ii1–54.

4. Shinohara S, Hanagiri T, Takenaka M, Chikaishi Y, Oka S, Shimokawa H, et al. Evaluation of undiagnosed solitary lung nodules according to the probability of malignancy in the American College of Chest Physicians (ACCP) evidence-based clinical practice guidelines. Radiol Oncol. 2014;48(1):50–5.

5. MacMahon H, Naidich DP, Goo JM, Lee KS, Leung ANC, Mayo JR, et al. Guidelines for management of incidental pulmonary nodules detected on CT images: From the Fleischner Society 2017. Radiology. 2017;284(1):228–43.

6. Li F, Sone S, Abe H, MacMahon H, Armato SG, Doi K. Lung cancers missed at low-dose helical CT screening in a general population: Comparison of clinical, histopathologic, and imaging findings. Radiology. 2002;225(3):673–83.

7. Joo HO, Ie RY, Sung HK, Hyung SS, Soo KC. Clinical significance of small pulmonary nodules with little or no 18F-FDG uptake on PET/CT images of patients with nonthoracic malignancies. J Nucl Med. 2007;48(1):15–21.

8. Chen S, Harmon S, Perk T, Li X, Chen M, Li Y, et al. Diagnostic classification of solitary pulmonary nodules using dual time 18F-FDG PET/CT image texture

features in granuloma-endemic regions. Sci Rep. 2017;7(1).

9. Wilson R, Devaraj A. Radiomics of pulmonary nodules and lung cancer. Vol. 6, Translational Lung Cancer Research. 2017. p. 86–91.

10. Hawkins S, Wang H, Liu Y, Garcia A, Stringfield O, Krewer H, et al. Predicting Malignant Nodules from Screening CT Scans. J Thorac Oncol. 2016;11(12):2120–8.

11. Xu Y, Lu L, Lin-Ning E, Lian W, Yang H, Schwartz LH, et al. Application of radiomics in predicting the malignancy of pulmonary nodules in different sizes. Am J Roentgenol. 2019;213(6):1213–20.

12. Ather S, Kadir T, Gleeson F. Artificial intelligence and radiomics in pulmonary nodule management: current status and future applications. Vol. 75, Clinical Radiology. 2020. p. 13–9.

13. Khawaja A, Bartholmai BJ, Rajagopalan S, Karwoski RA, Varghese C, Maldonado F, et al. Do we need to see to believe?—radiomics for lung nodule classification and lung cancer risk stratification. Vol. 12, Journal of Thoracic Disease. 2020. p. 3303–16.

14. Feng B, Chen X, Chen Y, Liu K, Li K, Liu X, et al. Radiomics nomogram for preoperative differentiation of lung tuberculoma from adenocarcinoma in solitary pulmonary solid nodule. Eur J Radiol. 2020;128.

15. Palumbo B, Bianconi F, Palumbo I, Fravolini ML, Minestrini M, Nuvoli S, et al. Value of Shape and Texture Features from 18F-FDG PET/CT to Discriminate between Benign and Malignant Solitary Pulmonary Nodules: An Experimental Evaluation. Diagnostics. 2020;10(9).

16. Henschke CI, Yankelevitz DF, Yip R, Reeves AP, Farooqi A, Xu D, et al. Lung

391 cancers diagnosed at annual CT screening: Volume doubling times.
392 Radiology. 2012;263(2):578–83.

393 17. Koroscil MT, Bowman MH, Morris MJ, Skabelund AJ, Hersh AM. Effect of a
394 pulmonary nodule fact sheet on patient anxiety and knowledge: A quality
395 improvement initiative. BMJ Open Qual. 2018;7(3).

396 18. Slatore CG, Wiener RS, Golden SE, Au DH, Ganzini L. Longitudinal
397 assessment of distress among veterans with incidental pulmonary nodules.
398 Ann Am Thorac Soc. 2016;13(11):1983–91.

399 19. Cronin P, Dwamena BA, Kelly AM, Carlos RC. Solitary pulmonary nodules:
400 Meta-analytic comparison of cross-sectional imaging modalities for diagnosis
401 of malignancy. Radiology. 2008 Mar;246(3):772–82.

402 20. Wu CC, Maher MM, Shepard JAO. Complications of CT-guided percutaneous
403 needle biopsy of the chest: Prevention and management. Vol. 196, American
404 Journal of Roentgenology. 2011.

405 21. Huang M De, Weng HH, Hsu SL, Hsu LS, Lin WM, Chen CW, et al. Accuracy
406 and complications of CT-guided pulmonary core biopsy in small nodules: A
407 single-center experience. Cancer Imaging. 2019;19(1).

408 22. Folkman J. How is blood vessel growth regulated in normal and neoplastic
409 tissue?—G. H. A. clowes memorial award lecture. Cancer Res.
410 1986;46(2):467–73.

411 23. Cavalcanti PG, Shirani S, Scharcanski J, Fong C, Meng J, Castelli J, et al.
412 Lung nodule segmentation in chest computed tomography using a novel
413 background estimation method. Quant Imaging Med Surg. 2016;6(1):16–24.

414 24. Ohno Y, Nishio M, Koyama H, Seki S, Tsubakimoto M, Fujisawa Y, et al.

Solitary pulmonary nodules: Comparison of dynamic first-pass contrast-enhanced perfusion area-detector CT, dynamic first-pass contrast-enhanced MR imaging, and FDG PET/CT. Radiology. 2015;274(2):563–75.

25. Ohno Y, Nishio M, Koyama H, Miura S, Yoshikawa T, Matsumoto S, et al. Dynamic contrast-enhanced CT and MRI for pulmonary nodule assessment. Am J Roentgenol. 2014;202(3):515–29.

26. Huang YE, Lu HI, Liu FY, Huang YJ, Lin MC, Chen CF, et al. Solitary pulmonary nodules differentiated by Dynamic F-18 FDG PET in a region with high prevalence of granulomatous disease. J Radiat Res. 2012 Jan;53(2):306–12.

27. Yuan X, Zhang J, Quan C, Cao J, Ao G, Tian Y, et al. Differentiation of malignant and benign pulmonary nodules with first-pass dual-input perfusion CT. Eur Radiol. 2013;23(9):2469–74.

28. Ohno Y, Koyama H, Fujisawa Y, Yoshikawa T, Seki S, Sugihara N, et al. Dynamic contrast-enhanced perfusion area detector CT for non-small cell lung cancer patients: Influence of mathematical models on early prediction capabilities for treatment response and recurrence after chemoradiotherapy. Eur J Radiol. 2016 Jan;85(1):176–86.

29. Ohno Y, Nishio M, Koyama H, Fujisawa Y, Yoshikawa T, Matsumoto S, et al. Comparison of quantitatively analyzed dynamic area-detector CT using various mathematic methods with FDG PET/CT in management of solitary pulmonary nodules. Am J Roentgenol. 2013;200(6).

30. Karakatsanis NA, Lodge MA, Tahari AK, Zhou Y, Wahl RL, Rahmim A. Dynamic whole-body PET parametric imaging: I. Concept, acquisition protocol optimization and clinical application. Phys Med Biol. 2013 Oct 21;58(20):7391–

418.

31. Dimitrakopoulou-Strauss A, Pan L, Strauss LG. Quantitative approaches of dynamic FDG-PET and PET/CT studies (dPET/CT) for the evaluation of oncological patients. Cancer Imaging. 2012 Jan;12:283–9.

32. Yi CA, Kyung SL, Kim BT, Joon YC, Kwon OJ, Kim H, et al. Tissue characterization of solitary pulmonary nodule: Comparative study between helical dynamic CT and integrated PET/CT. J Nucl Med. 2006;47(3):443–50.

33. Ohno Y, Koyama H, Matsumoto K, Onishi Y, Takenaka D, Fujisawa Y, et al. Differentiation of malignant and benign pulmonary nodules with quantitative first-pass 320-detector row perfusion CT versus FDG PET/CT. Radiology. 2011 Feb 1;258(2):599–609.

34. Mirsadraee S, Reid JH, Connell M, MacNee W, Hirani N, Murchison JT, et al. Dynamic (4D) CT perfusion offers simultaneous functional and anatomical insights into pulmonary embolism resolution. Eur J Radiol. 2016;85(10):1883–90.

35. Patlak CS, Blasberg RG, Fenstermacher JD. Graphical evaluation of blood-to-brain transfer constants from multiple-time uptake data. J Cereb Blood Flow Metab. 1983;3(1):1–7.

36. Evangelista L, Cuocolo A, Pace L, Mansi L, Del Vecchio S, Miletto P, et al. Performance of FDG-PET/CT in solitary pulmonary nodule based on pre-test likelihood of malignancy: results from the ITALIAN retrospective multicenter trial. Eur J Nucl Med Mol Imaging. 2018;45(11):1898–907.

37. Weir-McCall JR, Harris S, Miles KA, Qureshi NR, Rintoul RC, Dizdarevic S, et al. Impact of solitary pulmonary nodule size on qualitative and quantitative assessment using 18F-fluorodeoxyglucose PET/CT: the SPUTNIK trial. Eur J

Nucl Med Mol Imaging. 2020;

38. Sim YT, Poon FW. Imaging of solitary pulmonary nodule-a clinical review. Quant Imaging Med Surg. 2013;3(6):316–26.

39. Ambrosini V, Nicolini S, Caroli P, Nanni C, Massaro A, Marzola MC, et al. PET/CT imaging in different types of lung cancer: An overview. Vol. 81, European Journal of Radiology. 2012. p. 988–1001.

40. Chen CJ, Lee BF, Yao WJ, Cheng L, Wu PS, Ching LC, et al. Dual-phase 18F-FDG PET in the diagnosis of pulmonary nodules with an initial standard uptake value less than 2.5. Am J Roentgenol. 2008 Aug 23;191(2):475–9.

41. Cloran FJ, Banks KP, Song WS, Kim Y, Bradley YC. Limitations of dual time point PET in the assessment of lung nodules with low FDG avidity. Lung Cancer. 2010 Apr 1;68(1):66–71.

42. Chiu CH, Yeh YC, Lin KH, Wu YC, Lee YC, Chou TY, et al. Histological subtypes of lung adenocarcinoma have differential 18F-fluorodeoxyglucose uptakes on the positron emission tomography/computed tomography scan. J Thorac Oncol. 2011;6(10):1697–703.

43. Veronesi G, Bellomi M, Veronesi U, Paganelli G, Maisonneuve P, Scanagatta P, et al. Role of Positron Emission Tomography Scanning in the Management of Lung Nodules Detected at Baseline Computed Tomography Screening. Ann Thorac Surg. 2007;84(3):959–66.

44. Nomori H, Watanabe K, Ohtsuka T, Naruke T, Suemasu K, Uno K. Evaluation of F-18 fluorodeoxyglucose (FDG) PET scanning for pulmonary nodules less than 3 cm in diameter, with special reference to the CT images. Lung Cancer. 2004;45(1):19–27.

45. Berger KL, Nicholson SA, Dehdashti F, Siegel BA. FDG PET evaluation of mucinous neoplasms: Correlation of FDG uptake with histopathologic features. Am J Roentgenol. 2000;174(4):1005–8.

46. Yi CA, Lee KS, Kim EA, Han J, Kim H, Kwon OJ, et al. Solitary pulmonary nodules: Dynamic enhanced multi-detector row CT study and comparison with vascular endothelial growth factor and microvessel density. Radiology. 2004 Oct;233(1):191–9.

47. Zhang M, Kono M. Solitary pulmonary nodules: Evaluation of blood flow patterns with dynamic CT. Radiology. 1997 Nov;205(2):471–8.

48. Hornick JL, Fletcher CDM. PEComa: What do we know so far? Vol. 48, Histopathology. 2006. p. 75–82.

49. Stallmann S, Fisseler-Eckhoff A. Mesenchymale Tumoren der Lunge. Pneumologe. 2014;12(1):34–43.

50. Chakrabarti A, Bandyopadhyay M, Purkayastha B. Malignant perivascular epitheloid cell tumour (PEComa) of the lung-A rare entity. Innov Surg Sci. 2020;2(1):39–42.

51. Kim WJ, Kim SR, Choe YH, Lee KY, Park SJ, Lee HB, et al. Clear cell “sugar”tumor of the lung: A well-enhanced mass with an early washout pattern on dynamic contrast-enhanced computed tomography. J Korean Med Sci. 2008;23(6):1121–4.

52. Suljic A, Tomse P, Jensterle L, Skrk D. The impact of reconstruction algorithms and time of flight information on PET/CT image quality. Radiol Oncol. 2015;49(3):227–33.

53. Bhalla A, Das A, Naranje P, Irodi A, Raj V, Goyal A. Imaging protocols for CT

chest: A recommendation. Indian J Radiol Imaging. 2019;29(3):236.

54. Dolde K, Naumann P, Dávid C, Kachelriess M, Lomax AJ, Weber DC, et al. Comparing the effectiveness and efficiency of various gating approaches for PBS proton therapy of pancreatic cancer using 4D-MRI datasets. Phys Med Biol. 2019;64(8).

55. McCollough CH, Primak AN, Braun N, Kofler J, Yu L, Christner J. Strategies for Reducing Radiation Dose in CT. Vol. 47, Radiologic Clinics of North America. 2009. p. 27–40.

56. Qureshi NR, Rintoul RC, Miles KA, George S, Harris S, Madden J, et al. Accuracy and cost-effectiveness of dynamic contrast-enhanced CT in the characterisation of solitary pulmonary nodules — The SPUtNIk study. BMJ Open Respir Res. 2016;3(1).

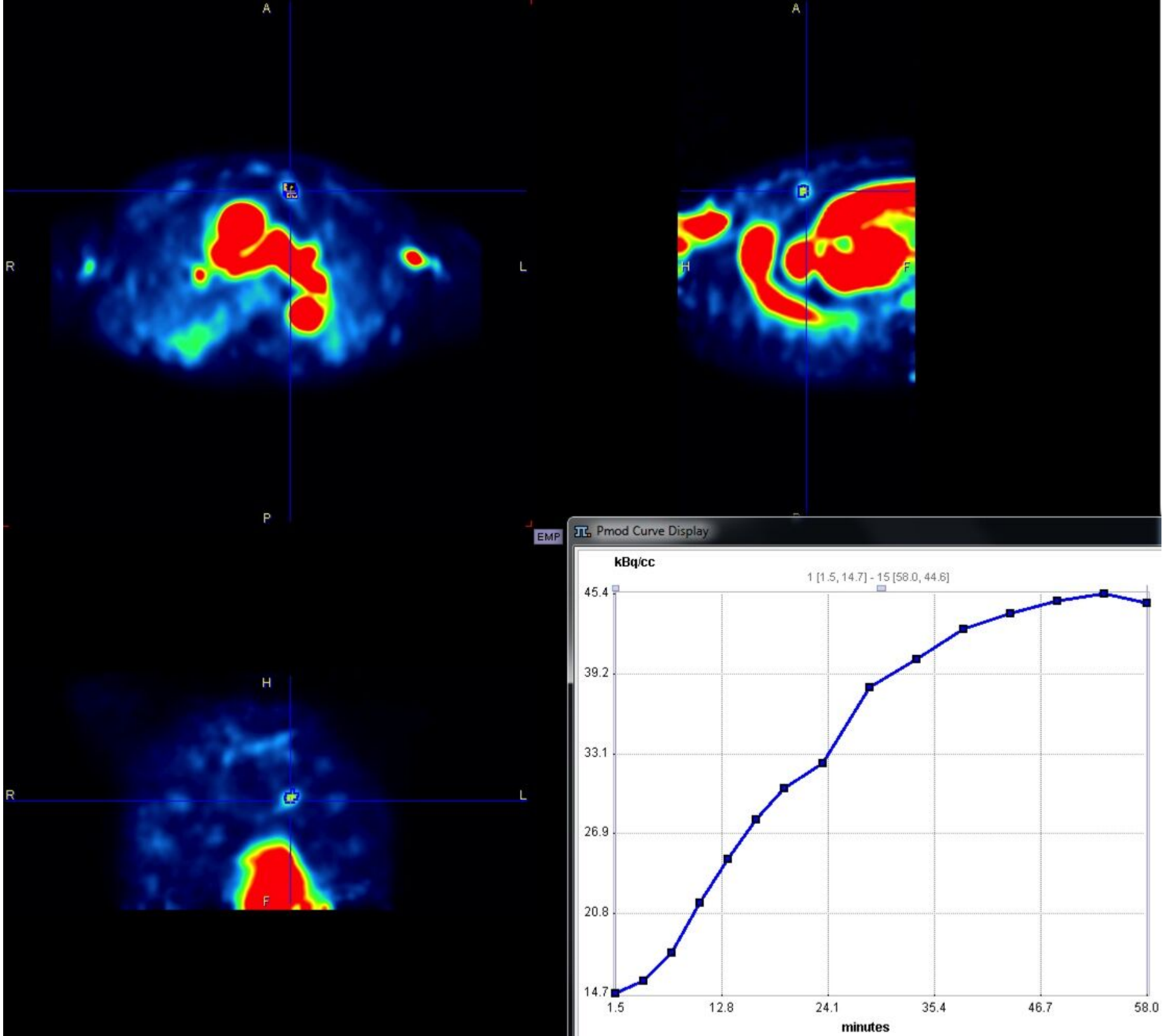
A
R
L
P
A
H
F
EMP
H
R
L
F
Pmod Curve Display
kBq/cc
1 [1.5, 14.7] - 15 [58.0, 44.6]
45.4
39.2
33.1
26.9
20.8
14.7
1.5
12.8
24.1
35.4
46.7
58.0
minutes

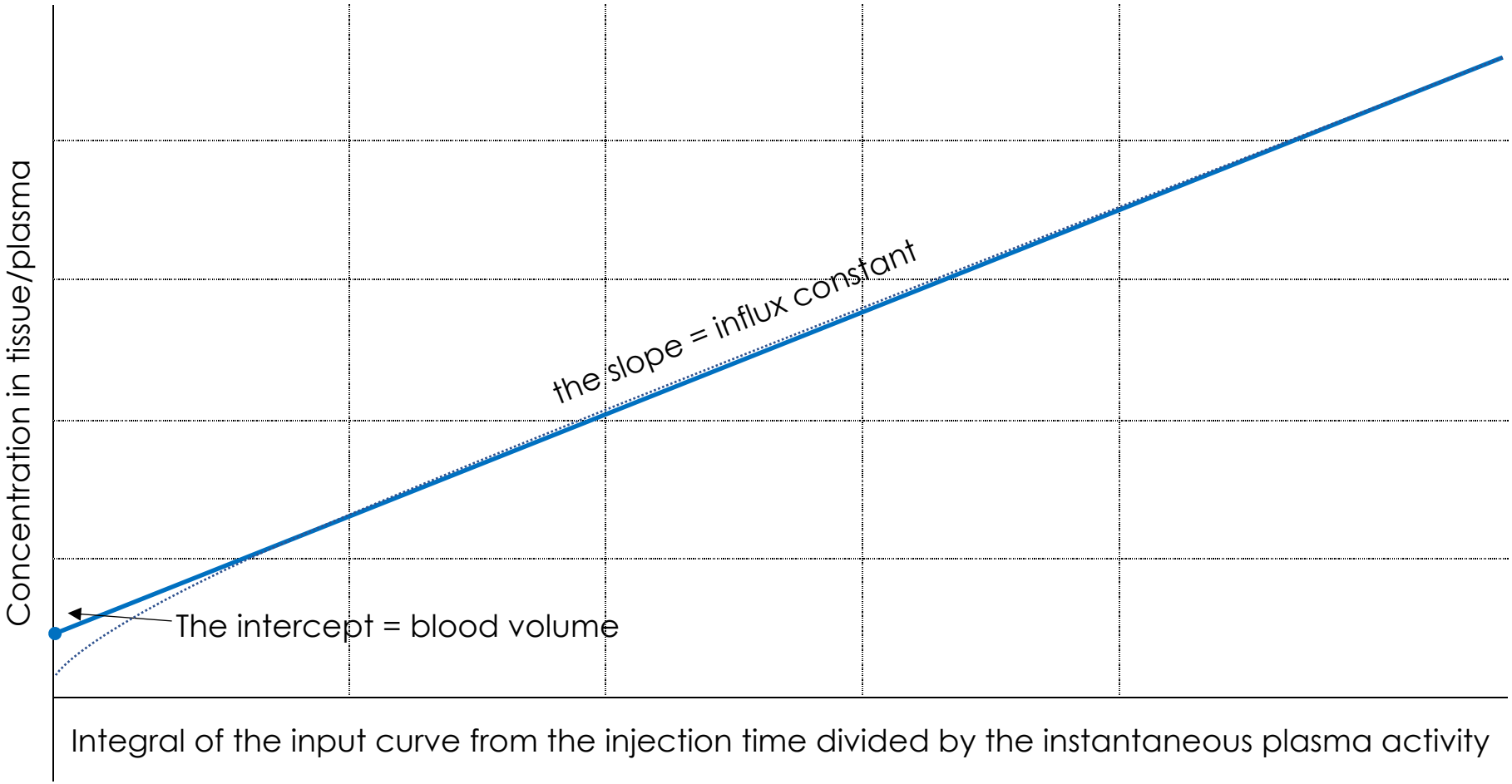
Concentration in tissue/plasma
the slope = influx constant
The intercept = blood volume
Integral of the input curve from the injection time divided by the instantaneous plasma activity

^{18}F-FDG PET/CT
SUV_{max}

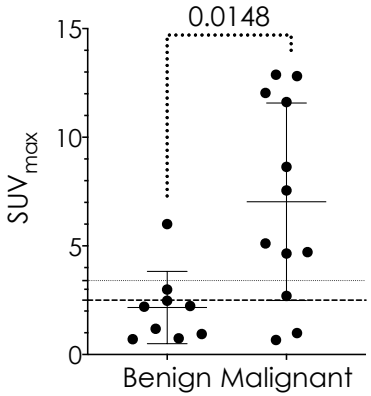

(a)

Dynamic ^{18}F-FDG PET/CT
K_i

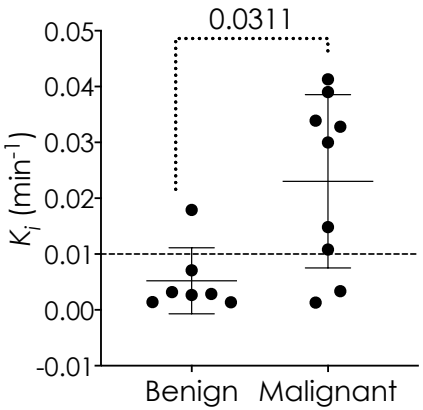

(b)

Perfusion CT
BV

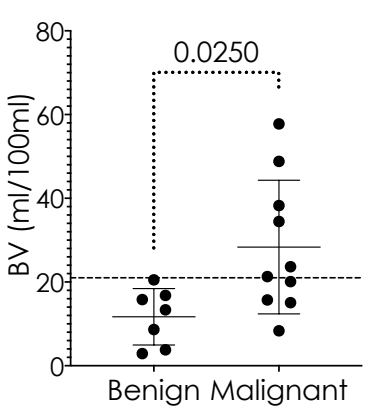

(c)

Perfusion CT
AF

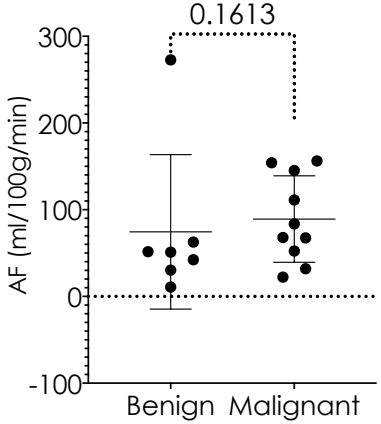

(d)

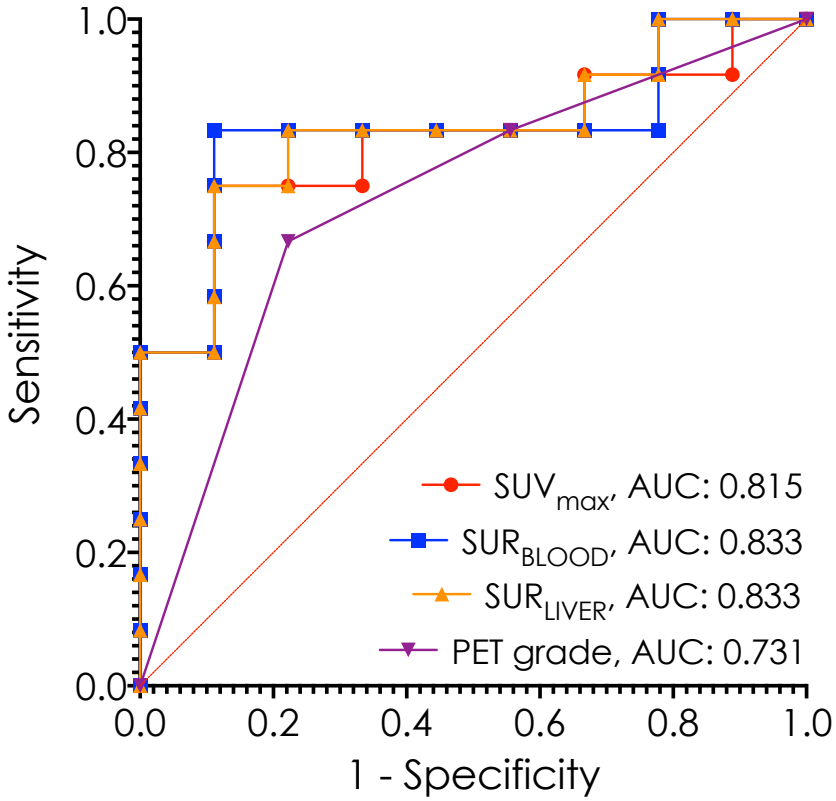
1.0
0.8
0.6
0.4
0.2
0.0
Sensitivity
0.0
0.2
0.4
0.6
0.8
1.0
1 - Specificity
SUV$_{max}$, AUC: 0.815
SUR$_{BLOOD}$, AUC: 0.833
SUR$_{LIVER}$, AUC: 0.833
PET grade, AUC: 0.731

(a)

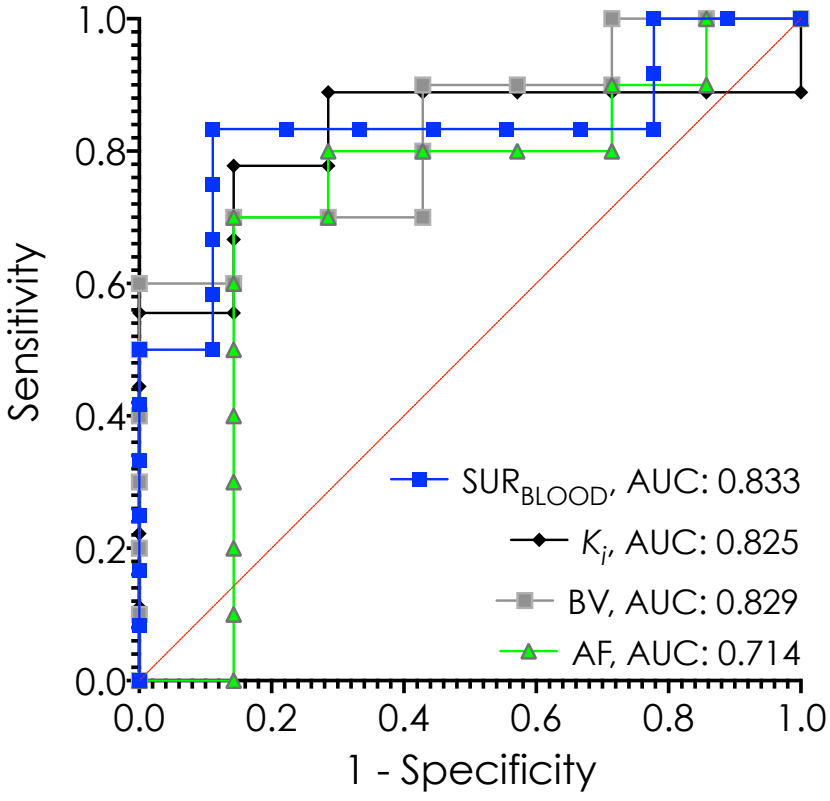
1.0
0.8
0.6
0.4
0.2
0.0
Sensitivity
0.0
0.2
0.4
0.6
0.8
1.0
1 - Specificity
SUR$_{BLOOD}$, AUC: 0.833
K_i, AUC: 0.825
BV, AUC: 0.829
AF, AUC: 0.714

(b)

TABLE 1. The demographic data, average nodule size, SUV_{max}, metabolic parameter relating to the pulmonary nodules through dynamic ^{18}F-FDG PET/CT, and perfusion parameters through perfusion CT for the benign and malignant nodules.

	Benign Nodules	Malignant Nodules	p value
Total Number of nodules	9	12	
Number of male patients (%)	5/9 (55 %)	6/12 (50 %)	
Average patient age (years ± SD)	63±7.5	68±6.7	
Average nodule size, Range (mm)	18, 9–29	22, 12–30	
Average SUV_{max} ^{18}F-FDG PET/CT ± SD	2.2±1.7	7.0±4.5	0.0148
Number of nodules analysed for dynamic ^{18}F-FDG PET/CT	7	9	
Average K_i ± SD (min^{-1})	0.0057±0.0071	0.0230±0.0155	0.0311
Number of nodules analysed for perfusion CT parameters	7	10	
Average BV ± SD (Patlak, ml/100ml)	11.6857±6.7347	28.3400±15.9672	0.0250
Average AF ± SD (ml/100g/min)	74.4571±89.0321	89.2000±49.8883	0.1613

TABLE 2. Comparison of the diagnostic accuracy of different techniques and parameters with pre-specified and derived cut-point values for malignancy.

Parameter	Cut-point value/grade		Sensitivity (95% CI)	Specificity (95% CI)	Accuracy
SUV_{max}	Pre-specified	≥2.5*	75.0% (46.8 to 91.1%)	66.7% (35.4 to 87.9%)	71.4%
	Derived	≥3.4	75.0% (46.8 to 91.1%)	88.9% (56.5 to 99.43%)	81.0%
SUR_{BLOOD}	Pre-specified	≥1.56	83.3% (55.2 to 97.0%)	88.9% (56.5 to 99.4%)	85.7%
	Derived				
SUR_{LIVER}	Pre-specified	≥1.12	83.3% (55.2 to 97.0%)	66.7% (35.4 to 87.9%)	76.2%
	Derived	≥1.65	75% (46.8 to 91.1%)	88.9% (56.5 to 99.4%)	81.0%
SUV grade	Pre-specified & Derived	≥3	66.7% (39.0 to 86.2%)	77.8% (45.3 to 96.0%)	71.4%
K_i	Derived	≥0.01 min^{-1}	77.8% (45.2 to 96.0%)	85.7% (48.7 to 99.3%)	81.3%
BV	Derived	≥21 ml/100ml	70% (39.7 to 89.2%)	100% (64.6 to 100%)	82.4%
AF	Derived	≥65 ml/100g/min	70% (39.7 to 89.2%)	85.7% (48.7 to 99.3%)	76.5%

* adding cut-points SUV_{max} ≥1.75 and ≥3.6 for nodules <12 mm and >16 mm, respectvely,[37] resulted in sensitivity, specificity and accuracy of 72.7%, 70.0% and 71.4%, respectively.